

ATC: An Image-based Atmospheric Correction Software in MATLAB and SML

Jaewon Choi*, Joong-Sun Won[†], and Saro Lee**[†]

*Department of Earth System Sciences, Yonsei University, 134 Shinchon-dong, Seodaemun-gu, Seoul 120-749, Korea

**Geoscience Information Center, Korea Institute of Geoscience and Mineral Resources (KIGAM), 30,

Gajung-dong, Yusong-gu, Daejeon, 305-350, Korea

Abstract : An image-based atmospheric correction software ATC is implemented using MATLAB and SML (Spatial Modeler Language in ERDAS IMAGINE). and it was tested using Landsat TM/ETM+ data. This ATC has two main functional modules, which are composed of a semiautomatic type and an automatic type. The semi-automatic functional module includes the Julian day (JD), Earth-Sun distance (ESD), solar zenith angle (SZA) and path radiance (PR), which are programmed as individual small functions. For the automatic functional module, these parameters are computed by using the header file of Landsat TM/ETM+. Three atmospheric correction algorithms are included: The apparent reflectance model (AR), one-percent dark object subtraction technique (DOS), and cosine approximation model (COST). The ACT is efficient as well as easy to use in a system with MATLAB and SML.

Key Words : Image-based atmospheric correction, Landsat TM/ETM+, AR model, DOS model, COST model, MATLAB/SML.

1. Introduction

There are several ways to correct atmospheric effects of optical remote sensor data. Some are relatively straightforward while others are complicated, being founded on physical principles and requiring a significant amount of information to function properly (Cracknell and Hayes, 1993). Absolute atmospheric correction often has relatively high accuracy, and it requires *in situ* measurements of state and composition of the atmospheric profile at the time of satellite overflight such as spectral optical

thickness of various atmospheric components. However, these measurements are practically near impossible to obtain, and the procedures involved are too expensive to use operationally. The one-percent DOS technique (Moran *et al.*, 1992) and the COST model (Chavez, 1996) image-based atmospheric correction methods have been proposed to simplify atmospheric correction. These methods have also been evaluated by several authors in areas characterized by relatively low humidity (Chavez, 1996; Moran *et al.*, 1992). The main advantages of these models are that they are strictly image-based

Received September 27, 2008; Revised October 7, 2008; Accepted October 14, 2008.

[†] Corresponding Author: Saro Lee (leesaro@kigam.re.kr)

procedures and therefore do not require *in situ* field measurements and they are simple and very straightforward to apply (Chavez, 1996).

MATLAB is a powerful programming language for software development. The language is easy to learn and contains a large collection of mathematical functions that facilitate the task of writing complicated code, including graphical user interfaces (GUIs). However, it has limitations including speed and memory consumption. The Spatial Modeler Language (SML) in ERDAS IMAGINE is a script language that is designed for GIS modeling and image-processing applications. The SML is able to define simple or complex processing operations outside of Model Maker, the GUI in the Spatial Modeler component.

Here we introduce an implemented software named ATmospheric Correction (ATC) for image-based atmospheric correction based on the models of AR (Chavez, 1996), the one-percent DOS (Moran *et al.*, 1992) and COST (Chavez, 1996). The software was tested using Landsat TM/ETM+. Although ATC was implemented under different MATLAB and SML language environment, it was programmed for optimizing advantages of both languages including GUIs.

2. Background

Provided that sky irradiance is isotropic and only atmospheric scattering and absorption are considered, the general equation of spectral reflectance of the surface can be expressed as (Moran *et al.*, 1992):

$$REF = \frac{\pi \cdot (L_{\lambda} - L_{haze}) \cdot d^2}{TAU_v \cdot (ESUN_{\lambda} \cdot \cos\theta_s \cdot TAU_z + E_{down})}, \quad (1)$$

where REF is spectral reflectance of the surface; L_{λ} is spectral radiance at the sensor's aperture; L_{haze} is the

upwelling atmospheric spectral radiance scattered in the direction of and at the sensor entrance pupil and within the sensor's field of view [$W \cdot m^{-2} \cdot sr^{-1} \cdot \mu m^{-1}$], *i.e.*, the path radiance; d is the earth-sun distance in astronomical units; TAU_v is atmospheric transmittance along the path on the ground surface to the sensor; $ESUN_{\lambda}$ is the mean solar exoatmospheric irradiance; θ_s is the solar zenith angle in degrees; TAU_z is the atmospheric transmittance along the path from the sun to the ground surface; E_{down} is downwelling spectral irradiance at the surface due to the scattered solar flux in the atmosphere [$W \cdot m^{-2} \cdot \mu m^{-1}$].

1) Apparent reflectance (AR) model

The AR model assumes a unit atmospheric transmittance and neglect downwelling and scattering due to path radiance ($TAU_z = TAU_v = 1$, $E_{down} = L_{haze} = 0$). Then Eq. (1) is simplified to the following:

$$REF = \frac{\pi \cdot (L_{\lambda}) \cdot d^2}{(ESUN_{\lambda} \cdot \cos\theta_s)}, \quad (2)$$

2) One-percent DOS model

The atmosphere-scattered path radiance can be estimated with a relative spectral scattering DOS model under clear (λ^{-2}) atmospheric conditions (Chavez, 1988). Dark objects within the image are identified by an area with clear water in deep lakes or by the histogram method, which selects the haze DN value from the DN frequency histogram of a digital image (Chavez, 1988). The one-percent DOS technique was applied to estimate the difference between path radiance from these dark objects and the radiance from surfaces with 1% reflectance (Moran *et al.*, 1992). The scattering due to the path radiance term (L_{haze}) was only considered to compute spectral reflectance of the surface, and atmospheric transmittance and downwelling terms were ignored

($TAU_z = TAU_v = 1, Edown = 0$). Thus, Eq. (1) is simplified to:

$$REF = \frac{\pi \cdot (L_\lambda - L_{haze}) \cdot d^2}{(ESUN_\lambda \cdot \cos\theta_s)}, \quad (3)$$

3) COST model

According to Chavez (1996), the atmospheric transmittance terms (TAU_z, TAU_v) are computed by the cosine of the solar zenith angle where TAU_v has a value of 1.0 because it is zero degrees for nadir view. The scattering due to the path radiance term (L_{haze}) is derived by the dark object criteria and the downwelling term ($Edown$) is ignored. Therefore, Eq. (1) can be expressed as:

$$REF = \frac{\pi \cdot (L_\lambda - L_{haze}) \cdot d^2}{(ESUN_\lambda \cdot \cos\theta_s \cdot \cos\theta_s)}, \quad (4)$$

3. Program and guidance of the software tools

The program was implemented under MATLAB and SML environment and can be run on Microsoft Windows systems. There are two main modules: one is a semi-automatic image-based atmospheric correction module, and the other an automatic image-based atmospheric correction module. Fig. 1 is the flowchart of the software tool. For the atmospheric correction, four input parameters are required as in Fig. 1 including Julian day (JD), Earth-Sun distance (ESD), solar zenith angle (SZA) and path radiance (PR). The main difference between the semi-automatic and automatic modules lies on the source of input parameters. The semi-automatic module employs an interactive calculation of the input parameters, while the automatic module imports and calculates them directly from Landsat TM/ETM+

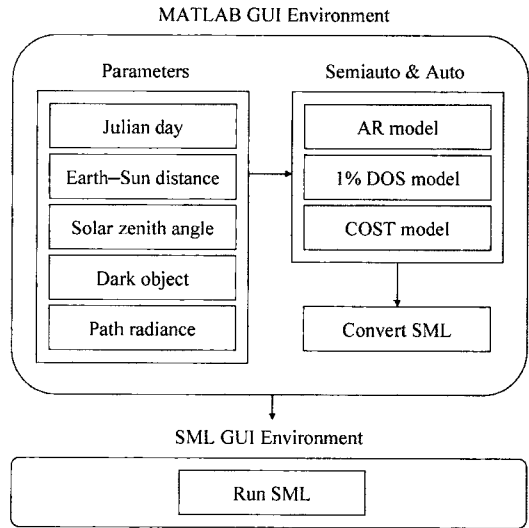


Fig. 1. Flowchart for software.

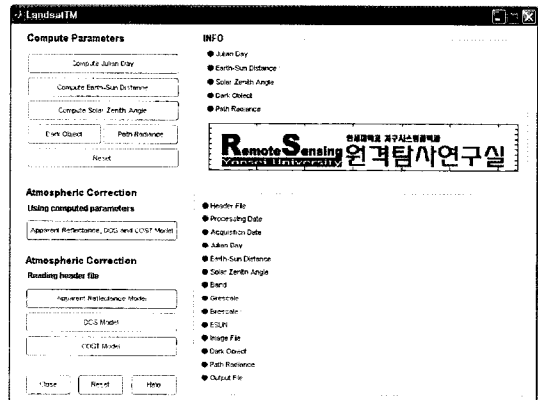


Fig. 2. Main menu of program.

header information. Fig. 2 shows a main menu window of the program. All parameters used in the program can be directly or indirectly input through the interface, and the input image file format is so far limited to the GeoTIFF.

1) Julian day

This is a sub-function of the image-based atmospheric correction software tool. It is a sub-category of the “Compute Parameters” group, and can be run by “Compute Julian day” button. Two input parameters of “month” and “day” are required.

2) Earth-Sun distance

The Earth-Sun distance is computed from the Julian day. It also belongs to the Compute Parameters group, and can be run by the button of "Compute Earth-Sun distance." It has one input value, the Julian day.

3) Solar zenith angle

The solar zenith angle is computed from the sun elevation angle. It is a sub-category of the Compute Parameters group, and can be run by "Solar zenith angle" button with an input value of the sun elevation angle.

4) Dark object

A dark object is identified by the histogram method that selects a haze digital number (DN) value from the DN frequency histogram of a digital image (Chavez, 1988). It is also a part of the Compute Parameters group and is run by the button of "Dark object." This function needs an input digital image. The ACT is so far only possible to import GeoTIFF formatted image data.

5) Path radiance

The scattering due to path radiance is computed from the dark object by subtracting the radiance from surfaces with 1% reflectance (Moran *et al.*, 1992). It

is in the Compute Parameters group and can be run by the button of "Path radiance." It has three input parameters of "Grescale", "Brescale", and "ESUN." Table 1 summarizes the band-specific rescaling gain (Grescale) and biases (Brescale) that the users will need to the digital number (Qcal) to spectral radiance (L_λ) (Chander G. *et al.*, 2007). The path radiance can only be computed after determining the parameters Julian day, Earth-Sun distance, solar zenith angle and dark object.

6) Reset

This button resets all information in "INFO" Which displays the resulting process.

7) Atmospheric correction using computed parameters

The button "Atmospheric correction using computed parameters" button group initiates calculation of correction values by the AR, one-percent DOS and COST models using the determined parameters. This button brings up the "Landsat TM1" window (Fig. 3a). It comprises two tables and six input values that can be run from each model. The first table in the "Landsat TM1" window shows rescaling gains and biases used for the conversion of L1-calibrated data product digital numbers (Qcal) to spectral radiance (L_λ) (Chander *et al.*, 2007), and the

Table 1. Rescaling gain and biases for Landsat 5

Rescaling Gain (Grescale) and Bias (Brescale)								
Processing Date	Mar 1, 84-May 4, 03		May 5, 03-Apr 1, 07		Apr 2, 07-Present			
Acquisition Date	Mar 1, 84-May 4, 03		Mar 1, 84-Apr 1, 07		Mar 1, 84-Dec 31, 91		Jan 1, 92-Present	
Band	Grescale	Brescale	Grescale	Brescale	Grescale	Brescale	Grescale	Brescale
1	0.602431	-1.52	0.762824	-1.52	0.668706	-1.52	0.762824	-1.52
2	1.175100	-2.84	1.442510	-2.84	1.317020	-2.84	1.442510	-2.84
3	0.805765	-1.17	1.039880	-1.17	1.039880	-1.17	1.039880	-1.17
4	0.814549	-1.51	0.872588	-1.51	0.872588	-1.51	0.872588	-1.51
5	0.108078	-0.37	0.119882	-0.37	0.119882	-0.37	0.119882	-0.37
6	0.055158	1.2378	0.055158	1.2378	0.055158	1.2378	0.055158	1.2378
7	0.056980	-0.15	0.065294	-0.15	0.065294	-0.15	0.065294	-0.15

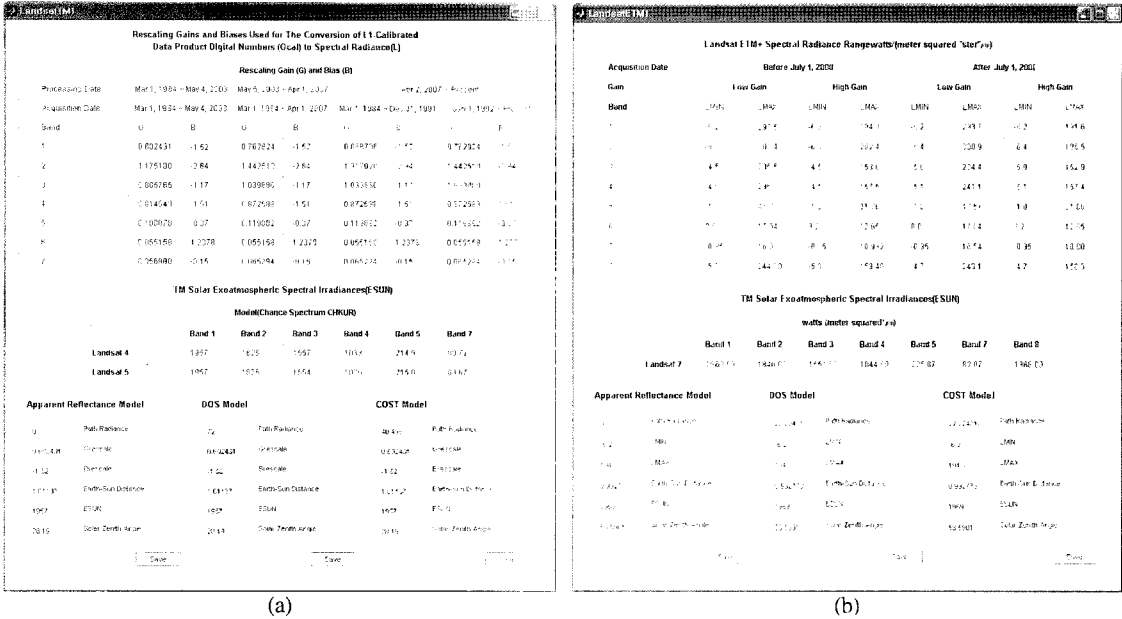


Fig. 3. "Landsat TM1/ETM1" window.

second table shows solar exoatmospheric spectral irradiances for Landsat 4 and 5 (Chander *et al.*, 2003). The path radiance, "Grescale", "Brescale", Earth-Sun distance, "ESUN" and the solar zenith angle were already computed for each model that can be saved from this window. The "Landsat ETM1" window is similar to the previous one but for Landsat ETM+ (Fig. 3b).

8) Atmospheric correction reading header file

The automatic module is collected in the "Atmospheric correction reading header file" group (the left bottom in Fig. 2). Three buttons for each AR, DOS and COST model are available. Input parameters for the calculation of the spectral reflectance are automatically imported and determined from the header file of Landsat TM/ETM+.

4. Example

1) Data preparation

A Landsat TM (path/row: 115/35) image dated 2 May 1992 and a Landsat ETM+ (path/row: 115/34) image dated 8 May 2000 were tested the performance of the software. These images are clipped for estimate, the same width and height of 105 km by 116 km. A systematical geometric and radiometric correction has already been performed to the image data to a quality level 1G, and the image file format is the GeoTIFF image format.

According to the meteorological data acquired from the Korea Meteorological Administration (KMA), the weather conditions and percent of cloud at the time the satellite passed were, respectively, clear sky and 0-2%. Water vapor information at the time the satellite passed could not be acquired from KMA. We assumed the "Mid-latitude summer" atmospheric model. Table 2 lists assumed atmospheric parameters in the example.

Table 2. Assumed atmospheric parameters in the examples

Parameters	
Atmosphere model	Mid-latitude summer (SAS) Water vapor: 2.92 g/cm ² Surface air temperature: 21 °C or 70 °C
Aerosol model	Tropospheric: visibility greater than 40km
Weather condition	Clear Scene visibility: 40 to 100km

2) Correction results

Landsat TM/ETM+ image data with bands 1, 2, 3 and 4 for image-based atmospheric correction were computed by the AR, one-percent DOS and COST model algorithm, and retrieved spectral reflectance values of the surface from each model were verified by the FLAASH module in the ENVI software.

In semiautomatic functional module, the first step is to compute parameters using the information recorded in the header file according to the description in Section 3. The resultant information of the Julian day, Earth-Sun distance, solar zenith angle, “dark object” and path radiance is shown by INFO in the main window (Table 3). The second step of the semiautomatic functional module is to compute the

spectral reflectance of the surface using the AR, one-percent DOS, and COST models. The final step of the semiautomatic functional module is similar to that in the automatic functional modules. Each *.mdl saved by each individual model was actually computed by the ERDAS Image software with SML.

The spectral reflectance of the surface retrieved by each individual model was verified by the result obtained from FLAASH in ENVI software. For comparative analysis, 30 random points were created, and the retrieved spectral reflectance values of the surface of band 1, 2, 3 and 4 were extracted by 30 random points. Scatter plots are shown for general comparison (Figs 4 and 5). These figures illustrate the differences of retrieved surface reflectance between individual model and FLAASH. Table 4 shows result of statistic analysis. In this table, positive value implies over corrected and negative value implies under corrected results. The one-percent DOS and COST model tend to under correct most of the reflectance, and the AR model shows negative and positive errors (Figs 4 and 5). As the results show, the COST model generated the best result. However, the

Table 3. Computed parameters for the examples

Landsat TM												
	AR model				DOS model				COST model			
	B1	B2	B3	B4	B1	B2	B3	B4	B1	B2	B3	B4
Path radiance	0	0	0	0	76	25	24	17	40.24	22.78	14.96	10.21
Grescale	0.60	1.17	0.80	0.81	0.60	1.17	0.80	0.81	0.60	1.17	0.80	0.81
Brescale	-1.52	-2.84	-1.17	-1.51	-1.52	-2.84	-1.17	-1.51	-1.52	-2.84	-1.17	-1.51
Earth-sun distance	1.00	1.00	1.00	1.00	1.00	1.00	1.00	1.00	1.00	1.00	1.00	1.00
ESUN	1957	1825	1557	1033	1957	1825	1557	1033	1957	1825	1557	1033
Solar zenith angle	35.92	35.92	35.92	35.92	35.92	35.92	35.92	35.92	35.92	35.92	35.92	35.92
Landsat ETM+												
Path radiance	0	0	0	0	63	43	30	11	38.53	24.65	10.90	3.28
LMIN	-6.2	-6	-4.5	-4.5	-6.2	-6	-4.5	-4.5	-6.2	-6	-4.5	-4.5
LMAX	194.3	202.4	158.6	235	194.3	202.4	158.6	235	194.3	202.4	158.6	235
Earth-sun distance	1.00	1.00	1.00	1.00	1.00	1.00	1.00	1.00	1.00	1.00	1.00	1.00
ESUN	1969	1840	1551	1044	1969	1840	1551	1044	1969	1840	1551	1044
Solar zenith angle	27.90	27.90	27.90	27.90	27.90	27.90	27.90	27.90	27.90	27.90	27.90	27.90

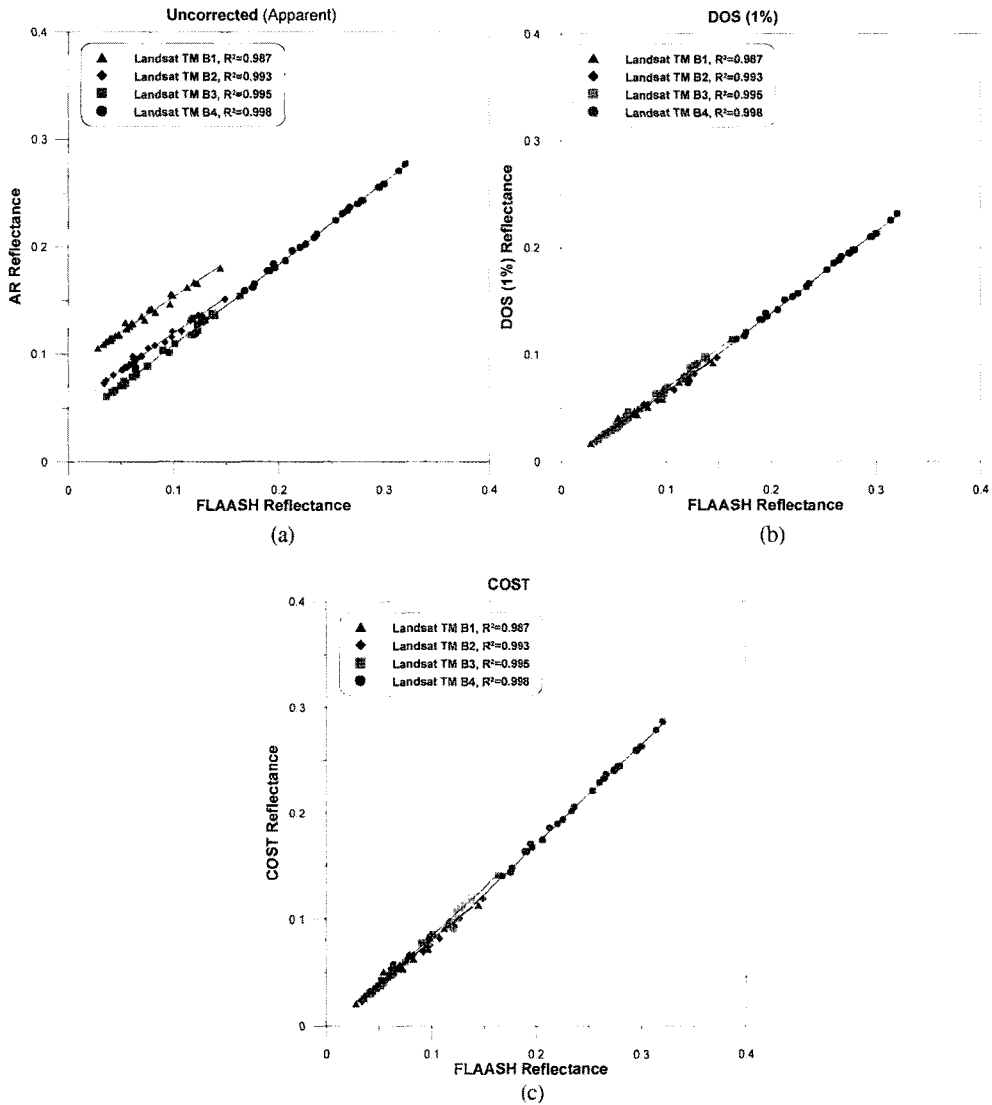


Fig. 4. These figures illustrate correlation and distribution between FLAASH reflectance and reflectance of individual mode using Landsat TM.

Table 4. Result of statistic analysis for differences of retrieved surface reflectance between individual model and FLAASH

	Landsat TM			Landsat ETM		
	AR	DOS (1%)	COST	AR	DOS (1%)	COST
Mean	-0.019	0.038	0.019	0.001	0.040	0.027
Standard deviation	0.035	0.023	0.009	0.049	0.037	0.033
Variance	0.001	0.001	0.000	0.002	0.001	0.001
Min	-0.076	0.012	0.004	-0.065	-0.034	-0.049
Max	0.043	0.089	0.037	0.157	0.168	0.138

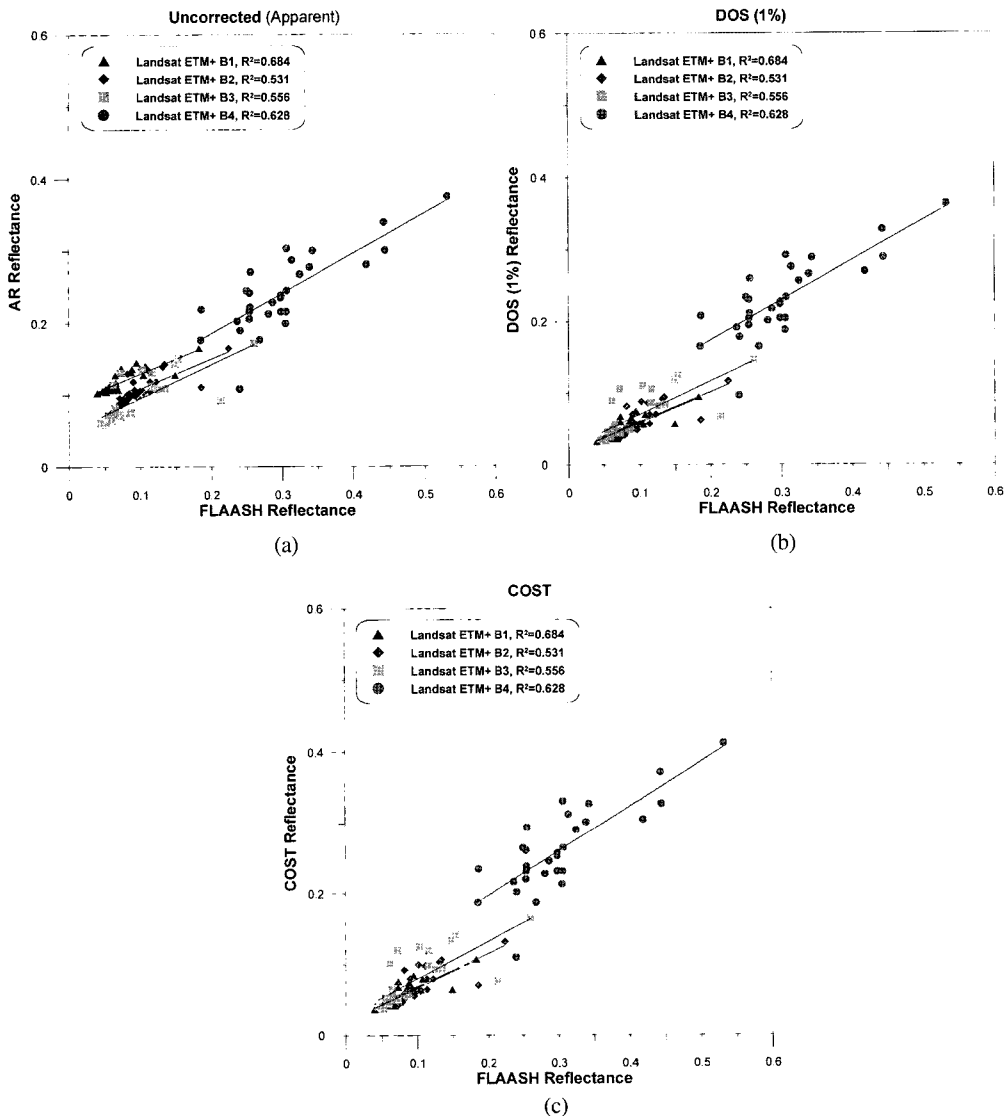


Fig. 5. These figures illustrate correlation and distribution between FLAASH reflectance and reflectance of individual model using Landsat ETM+.

result retrieved by the COST model applied to the Landsat ETM+ image shows a lower regression slope and Landsat TM image by FLAASH has a higher R-square value (Figs 4 and 5). Therefore, the dark object DN value for L_{haze} must be selected carefully (Chavez, 1996).

5. Conclusions

An image-based atmospheric correction tool was implemented under MATLAB and SML environment for Landsat TM/ETM+ data. This software tool provides three methods to retrieve spectral reflectance of the surface from Landsat TM/ETM+, which are the AR, one-percent DOS, and COST models. Each model with GUIs computes

correction parameters by semiautomatic or automatic functional modules. The precision of the spectral reflectance of the surface computed by this software tool follows the models and parameters used in the program. The implemented program is easy to learn and use.

References

- Chander, G. and B. Markham, 2003. Revised Landsat-5 TM radiometric calibration procedures and postcalibration dynamic ranges. *IEEE Transactions on Geoscience and Remote Sensing*, 41(11): 2674-2677.
- Chander, G., B. Markham, and J. Barsi, 2007. Revised Landsat-5 thematic mapper radiometric calibration. *IEEE Geoscience and Remote Sensing Letters*, 4(3): 490-494.
- Chavez, P. S. Jr., 1988. An improved dark-object subtraction technique for atmospheric scattering correction of multispectral data, *Remote Sensing of Environment*, 24: 459-479.
- Chavez, P. S. Jr., 1996. Image-based atmospheric corrections revisited and improved. *Photogrammetric Engineering & Remote Sensing*, 62(9): 1025-1036.
- Cracknell, A. P. and L. W. Hayes, 1993. Atmospheric corrections to passive satellite remote sensing data, In: *Introduction to Remote Sensing*, Taylor & Francis Press, London, pp. 116-158.
- Moran, M. S., R. D. Jackson, P. N. Slater, and P. M. Teillet, 1992. Evaluation of simplified procedures for retrieval of land surface reflectance factors from satellite sensor output. *Remote Sensing of Environment*, 41: 169-184.